

# Synthesis and Characterization of Wurtzite-Phase Copper Tin Selenide Nanocrystals

Michelle E. Norako, Matthew J. Greaney, and Richard L. Brutchey\*

Department of Chemistry and the Center for Energy Nanoscience and Technology, University of Southern California, Los Angeles, California 90089, United States

**S** Supporting Information

**ABSTRACT:** A new wurtzite phase of copper tin selenide (CTSe) was discovered, and the resulting nanocrystals were synthesized via a facile solution-phase method. The wurtzite CTSe nanocrystals were synthesized with dodecylamine and 1-dodecanethiol as coordinating solvents and di-*tert*-butyl diselenide ( ${}^t\text{Bu}_2\text{Se}_2$ ) as the selenium source. Specific reaction control (i.e., a combination of 1-dodecanethiol with  ${}^t\text{Bu}_2\text{Se}_2$ ) was proven to be critical in order to obtain this new phase of CTSe, which was verified by powder X-ray diffraction and selected area electron diffraction. The wurtzite CTSe nanocrystals possess an optical and electrochemical band gap of 1.7 eV and display an electrochemical photoresponse indicative of a p-type semiconductor.

The need for low-cost, scalable, and solution-processable photovoltaic materials is a leading impetus for new research in the field of semiconductor nanocrystal synthesis.<sup>1</sup> While great advancements in photovoltaic technologies have been made with CdTe, PbSe, and  $\text{CuIn}_x\text{Ga}_{1-x}\text{S}_2$  (CIGS) nanocrystals,<sup>2</sup> there is a current trend to replace materials containing environmentally harmful (e.g., Cd, Pb) and scarce (e.g., Te, In, Ga) elements with environmentally benign photovoltaic materials comprised of more earth abundant elements.<sup>3</sup> Along these lines, there has been a recent focus on the development of  $\text{Cu}_2\text{ZnSnS}_4$  (CZTS) and  $\text{Cu}_2\text{ZnSnSe}_4$  (CZTSe) nanocrystals,<sup>4</sup> in addition to the less compositionally complex binary tin monochalcogenide (SnS and SnSe) nanocrystals.<sup>5</sup> These materials all possess band gaps in the range of  $E_g = 1.3\text{--}1.6$  eV in addition to relatively high absorption coefficients ( $\sim 10^4$   $\text{cm}^{-1}$ ), which make them attractive candidates as absorber layers in photovoltaic devices.

Another potentially attractive, yet not well studied, material is  $\text{Cu}_2\text{SnSe}_3$  (copper tin selenide, CTSe). CTSe is a ternary I–IV–VI semiconductor that possesses a direct band gap in the range of  $E_g = 0.8\text{--}1.1$  eV, a high absorption coefficient ( $\sim 10^4\text{--}10^5$   $\text{cm}^{-1}$ ), and electron and hole mobilities on the order of  $\sim 2$  and  $\sim 870$   $\text{cm}^2 \text{V}^{-1} \text{s}^{-1}$ , respectively, for bulk material.<sup>6</sup> While it is often found as an impurity in CZTSe, there have been only a few examples where phase-pure CTSe has been prepared—as bulk single-crystals,<sup>7</sup> as thin films,<sup>6a,c,d</sup> and most recently in colloidal nanocrystal form.<sup>8</sup> These examples of CTSe were reported to crystallize in a cubic sphalerite-like phase ( $a = 5.69$  Å) or in a monoclinic phase with a sphalerite superstructure ( $a = 6.59$ ,  $b = 12.16$ , and  $c = 6.61$  Å;  $\beta = 108.6^\circ$ ).<sup>7c</sup> Since crystal

symmetry is known to influence the properties of materials, there have been a number of recent reports describing the use of kinetic control to determine crystal phase in nanocrystals. For example,  $\text{CuInS}_2$ ,  $\text{CuInSe}_2$ , and CIGS nanocrystals have been prepared in wurtzite and sphalerite crystal structures rather than the typical chalcopyrite structure.<sup>9</sup> Similarly, CZTS nanocrystals were recently reported in a wurtzite phase rather than the expected kesterite phase.<sup>10</sup> These investigations have shown that reaction control (including temperature, solvent, capping ligands, and chalcogenide source) is critical for crystal phase determination. Herein, we present the first report of a wurtzite phase for CTSe, in the form of colloidal nanocrystals, and establish its potential viability as a photovoltaic material by demonstrating clear electrochemical photocurrent upon illumination.

Diorganodichalcogenides have shown recent utility as facile and low-temperature chalcogenide sources for semiconductor nanocrystal syntheses.<sup>5a,9b,c,11</sup> Here, CTSe nanocrystals were synthesized via the fast addition of di-*tert*-butyl diselenide ( ${}^t\text{Bu}_2\text{Se}_2$ , 0.56 mmol) into a solution of CuCl (0.40 mmol) and  $\text{SnI}_4$  (0.20 mmol) in dodecylamine and 1-dodecanethiol (with or without oleic acid) at 180 °C, followed by heating for 5 min. The powder X-ray diffraction (XRD) pattern of the resulting CTSe nanocrystals did not match the diffraction pattern for previously reported CTSe nanocrystals or those in the JCPDS database (JCPDS no. 03-065-7524).<sup>7c</sup> A diffraction pattern was simulated starting from the wurtzite ZnSe crystal structure and substituting the  $\text{Zn}^{2+}$  lattice positions with a 2:1 occupancy probability of  $\text{Cu}^+$  and  $\text{Sn}^{4+}$  cations (see Supporting Information (SI)). The lattice constants calculated from the experimental diffraction pattern ( $a = 3.98$  and  $c = 6.66$  Å) were used in this simulation. The  $d$ -spacings of the experimentally observed reflections match well with the simulated reflections, suggesting that the CTSe nanocrystals adopt a wurtzite crystal structure (see Figure 1); however, the experimentally observed diffraction intensities match less well with the simulated diffraction pattern, likely because of the elemental non-stoichiometry in the CTSe nanocrystals (vide infra). Moreover, the variable diffraction peak widths suggest some degree of particle anisotropy. The major diffraction peaks can be indexed to the (100), (002), (101), (102), (110), (103), (112), (201), (202), and (203) reflections of the simulated wurtzite crystal structure. The (100), (101), (102), (103), (202), and (203) wurtzite reflections are distinct from cubic CTSe. There is a

Received: July 25, 2011

Published: December 8, 2011

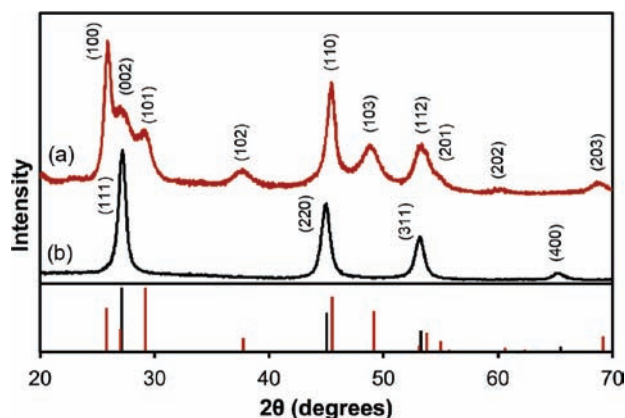


**Figure 1.** Experimental XRD patterns of (a) wurtzite and (b) cubic CTSe nanocrystals. The simulated XRD patterns of wurtzite (red) and cubic (black) CTSe are shown for reference.

significant  $2\theta$  shift between the second most intense reflections of each phase, which are (110) for wurtzite CTSe ( $2\theta \approx 45.6^\circ$ ) and (220) for cubic CTSe ( $2\theta \approx 44.8^\circ$ ). Therefore, if a significant amount of the cubic phase were present in the wurtzite CTSe, the shape of the diffraction maximum corresponding to the (110) reflection should be asymmetric, with a shoulder on the low angle side; however, such an asymmetry was not observed (see SI, Figure S1). This implies that if the cubic phase is present in the wurtzite CTSe, the amount is not significant by XRD analysis. Moreover, the (400) reflection of the cubic structure is distinct from the wurtzite structure and is not observed in the XRD pattern of wurtzite CTSe.

Specific reaction control is crucial to synthesize CTSe in the wurtzite phase. Under otherwise identical conditions, the nanocrystal synthesis without the addition of 1-dodecanethiol results in a phase-pure cubic CTSe product (Figure 1). Similar phenomena have recently been observed; that is, capping ligands have been shown to influence the formation of metastable crystal phases.<sup>12</sup> Interestingly, addition of increasing amounts of oleic acid (with 1-dodecanethiol and dodecylamine) appears to yield mainly cubic CTSe (see SI, Figure S2). When elemental selenium was substituted for  $\text{Bu}_2\text{Se}_2$  under otherwise identical conditions (i.e., equimolar based on selenium in the presence of 1-dodecanethiol and dodecylamine), a phase-impure cubic CTSe was produced (Figure S2). When TOPSe was used in an analogous way, phase-pure orthorhombic SnSe was formed, with no crystalline copper-containing phases being present (Figure S2). Thus, the chalcogenide source also seems to have a strong influence on phase determination. Preference for the wurtzite phase over the cubic phase appears to not be a direct result of any one component in this system; rather, it is a combination of variables (i.e., a particular combination of capping ligands and selenium source) that leads to phase determination.

The resulting CTSe nanocrystals have a mean diameter of  $15.1 \pm 2.9$  nm, as determined by TEM analysis (Figure 2). The lattice parameters calculated from selected area electron diffraction (SAED) patterns of several randomly chosen regions of the CTSe nanocrystals agree with the lattice parameters calculated from the XRD pattern for wurtzite CTSe. A high-resolution TEM (HRTEM) image of an apparent single-crystalline particle with the (002) lattice planes displayed ( $d = 3.26$  Å) is shown in Figure 2a. Energy dispersive X-ray

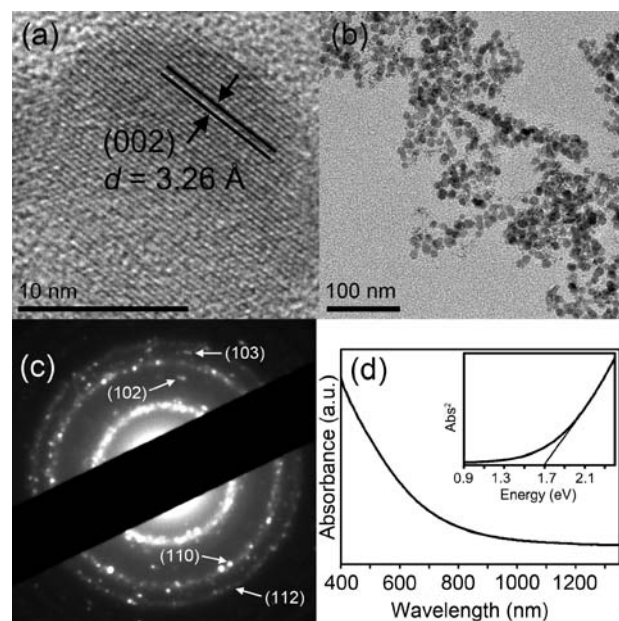


**Figure 2.** (a) HRTEM image of a CTSe nanocrystal with an interplanar spacing of 3.26 Å. (b) Low-resolution TEM image of CTSe nanocrystals with an average diameter of 15 nm. (c) SAED pattern of nanocrystals indexed to wurtzite CTSe. (d) UV-vis-NIR absorption spectrum of wurtzite CTSe nanocrystals.

spectroscopy (EDX) was used to analyze the elemental composition of the wurtzite CTSe nanocrystals (see SI, Figure S3). Analysis of several randomly selected areas gave an average Cu:Sn:Se composition of 1.57:0.92:3.00. This stoichiometry is slightly tin- and selenium-rich ( $\text{Cu}/\text{Sn} = 1.71$ ;  $\text{Se}/(\text{Cu} + \text{Sn}) = 1.14$ ) and deviates from the expected  $\text{Cu}_2\text{SnSe}_3$  stoichiometry; however, no additional crystalline phases of tin or selenium (e.g.,  $\text{SnSe}$  or  $\text{SnSe}_2$ ) were observed by XRD. The wurtzite CTSe nanocrystals absorb through the visible region of the solar spectrum, resulting in the black color of the material. UV-vis-NIR absorption spectroscopy was used to estimate a direct optical band gap of  $E_g = 1.7$  eV for the wurtzite CTSe nanocrystals (Figure 2d), which is higher than the values previously reported for cubic  $\text{Cu}_2\text{SnSe}_3$  thin films ( $E_g = 0.8\text{--}1.1$  eV).<sup>6a</sup> Interestingly, a direct optical band gap of  $E_g = 1.5$  eV was estimated for the colloidal cubic CTSe (see SI, Figure S4), suggesting that these nanocrystals are in the quantum confined regime.

Differential pulse voltammetry can be used to electrochemically estimate the band gap for semiconductor nanocrystals.<sup>13</sup> Differential pulse voltammograms (DPVs) of hydrazine-treated cubic and wurtzite CTSe nanocrystal films deposited on ITO are compared in Figure S5 (see SI). The separation between the  $E'_{\text{ox}}$  and  $E'_{\text{red}}$  peak onsets gives electrochemical band gaps of  $E_g = 1.5$  and 1.7 eV for the cubic and wurtzite nanocrystals, respectively, which is in agreement with the estimated optical band gaps. In the absence of hydrazine treatment, the as-made nanocrystals can be difficult to electrochemically characterize due to the insulating nature of the native capping ligands. It was found that briefly (20–30 s) dipping films of cubic or wurtzite CTSe in a 0.10 M hydrazine solution in acetonitrile enabled the collection of DPVs that appear much cleaner and possess stronger signals than those obtained without postdeposition hydrazine treatment.

To assess the potential applicability of the wurtzite CTSe nanocrystals as a photovoltaic material, the transient photocurrents of hydrazine-treated wurtzite CTSe nanocrystal films were evaluated in an aqueous photoelectrochemical cell containing 0.01 M  $\text{Eu}(\text{NO}_3)_3$  and 0.1 M KCl. Under illumination using a light-emitting diode with peak intensity of  $\lambda_{\text{max}} = 472$  nm, which is greater than the measured optical and electrochemical band gap, the nanocrystals produce a cathodic photocurrent that increases gradually with increasing negative potential (Figure 3), indicating that the wurtzite CTSe

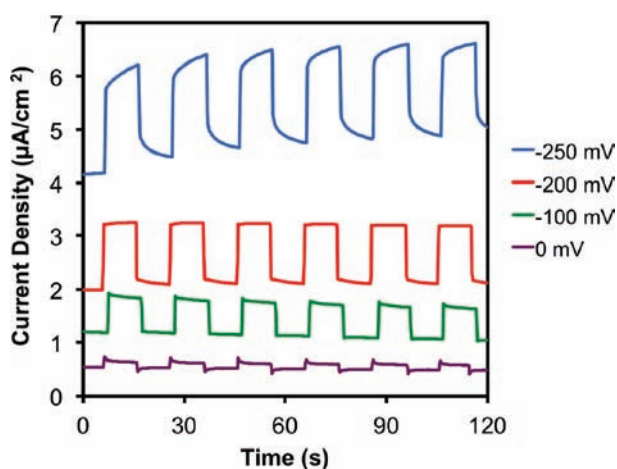


**Figure 3.** Transient photocurrent response of a wurtzite CTSe nanocrystal film showing clear p-type behavior. The nanocrystal film was spun-cast onto ITO and treated with hydrazine, and photocurrent was measured under nitrogen in aqueous 0.01 M  $\text{Eu}(\text{NO}_3)_3/0.1$  M KCl using 472 nm chopped illumination with a Ag wire pseudoreference electrode and a Pt wire counter electrode. The potential values are given relative to NHE.

nanocrystals exhibit p-type behavior.<sup>14</sup> For p-type semiconductors, electrons are transferred from the conduction band to a solution-phase oxidant and from the back ohmic contact into the semiconductor, resulting in the observation of cathodic currents. At 0 V bias vs NHE, the measured photocurrent is only  $0.10 \mu\text{A cm}^{-2}$  (measured as the difference between current density immediately prior to and at the end of an illumination cycle). As the bias was decreased to  $-250$  mV, the photocurrent increased more than an order of magnitude to  $1.8 \mu\text{A cm}^{-2}$ .

In summary, a facile synthesis of colloidal CTSe nanocrystals was described. Through a combination of 1-dodecanethiol capping ligands and a  $\text{Bu}_2\text{Se}_2$  selenium source, a metastable wurtzite phase of CTSe has been accessed for the first time. A direct band gap of  $E_g = 1.7$  eV matches reasonably well with the solar spectrum, making these nanocrystals potential candidates as photovoltaic materials. Indeed, preliminary experiments show that solution-deposited CTSe nanocrystal films exhibit a clear photoresponse. Future work will focus on examining the viability of this material for nanocrystal-based photovoltaic devices.

## ■ ASSOCIATED CONTENT

### Supporting Information

Experimental details; XRD patterns of material formed with the addition of oleic acid, elemental selenium, and TOPSe; EDX spectrum of wurtzite CTSe; UV–visible–NIR absorption spectrum of cubic CTSe; DPV curves for the wurtzite and

cubic CTSe nanocrystals. This material is available free of charge via the Internet at <http://pubs.acs.org>.

## ■ AUTHOR INFORMATION

### Corresponding Author

brutchey@usc.edu

## ■ ACKNOWLEDGMENTS

The material discovery is based on work supported by the National Science Foundation under DMR-0906745. M.E.N. and M.J.G. and the photoelectrochemical characterization were supported as part of the Center for Energy Nanoscience, an Energy Frontier Research Center funded by the U.S. Department of Energy, Office of Science, Office of Basic Energy Sciences, under Award No. DE-SC0001013. R.L.B. also acknowledges the Research Corporation for Science Advancement for a Cottrell Scholar Award.

## ■ REFERENCES

- (1) (a) Sargent, E. H. *Nat. Photonics* **2009**, *3*, 325. (b) Hillhouse, H. W.; Beard, M. C. *Curr. Opin. Colloid Interface Sci.* **2009**, *14*, 245. (c) Kamat, P. V. *J. Phys. Chem. C* **2008**, *112*, 18737.
- (2) (a) Gur, I.; Fromer, N. A.; Geier, M. L.; Alivisatos, A. P. *Science* **2005**, *310*, 462. (b) Luther, J. M.; Law, M.; Beard, M. C.; Song, Q.; Reese, M. O.; Ellingson, R. J.; Nozik, A. J. *Nano Lett.* **2008**, *8*, 3488. (c) Guo, Q.; Ford, G. M.; Hillhouse, H. W.; Agrawal, R. *Nano Lett.* **2009**, *9*, 3060.
- (3) (a) Wadia, C.; Alivisatos, A. P.; Kammen, D. M. *Environ. Sci. Technol.* **2009**, *43*, 2072. (b) Antunez, P. D.; Buckley, J. J.; Brutchey, R. L. *Nanoscale* **2011**, *3*, 2399.
- (4) (a) Riha, S. C.; Parkinson, B. A.; Prieto, A. L. *J. Am. Chem. Soc.* **2009**, *131*, 12054. (b) Steinhagen, C.; Panthani, M. G.; Akhavan, V.; Goodfellow, B.; Koo, B.; Korgel, B. A. *J. Am. Chem. Soc.* **2009**, *131*, 12554. (c) Guo, Q.; Hillhouse, H. W.; Agrawal, R. *J. Am. Chem. Soc.* **2009**, *131*, 11672.
- (5) (a) Franzman, M. A.; Schlenker, C. W.; Thompson, M. E.; Brutchey, R. L. *J. Am. Chem. Soc.* **2010**, *132*, 4060. (b) Baumgardner, W. J.; Choi, J. J.; Lim, Y.-F.; Hanrath, T. *J. Am. Chem. Soc.* **2010**, *132*, 9519. (c) Vaughn, D. D.; In, S.-I.; Schaak, R. E. *ACS Nano* **2011**, *5*, 8852. (d) Hickey, S. G.; Waurisch, C.; Rellinghaus, B.; Eychmuller, A. *J. Am. Chem. Soc.* **2008**, *130*, 14978. (e) Xu, Y.; Al-Salim, N.; Bumby, C. W.; Tilley, R. D. *J. Am. Chem. Soc.* **2009**, *131*, 15990.
- (6) (a) Babu, G. S.; Kumar, Y. B. K.; Reddy, Y. B. K.; Raja, V. S. *Mater. Chem. Phys.* **2006**, *96*, 442. (b) Berger, L. T.; Prochukhan, V. D. *Ternary Diamond-like Semiconductors*; Consultants Bureau: New York, 1969; pp 55–63. (c) Kuo, D.-H.; Haung, W.-D.; Huang, Y.-S.; Wu, J.-D.; Lin, Y.-J. *Thin Solid Films* **2010**, *518*, 7218. (d) Chandra, G. H.; Kumar, O. L.; Rao, R. P.; Uthanna, S. *J. Mater. Sci.* **2011**, *46*, 6952.
- (7) (a) Marcano, G.; Rincon, C.; de Chalbaud, L. M.; Bracho, D. B.; Sanchez Perez, G. *J. Appl. Phys.* **2001**, *90*, 1847. (b) Delgado, G. E.; Mora, A. J.; Marcano, G.; Rincon, C. *Mater. Res. Bull.* **2003**, *38*, 1949. (c) Marcano, G.; de Chalbaud, L. M.; Rincon, C.; Sanchez Perez, G. *Mater. Lett.* **2002**, *53*, 151.
- (8) Jeong, J.; Chung, H.; Ju, Y. C.; Moon, J.; Roh, J.; Yoon, S.; Do, Y. R.; Kim, W. *Mater. Lett.* **2010**, *64*, 2043.
- (9) (a) Pan, D.; An, L.; Sun, Z.; Hou, W.; Yang, Y.; Yang, Z.; Lu, Y. *J. Am. Chem. Soc.* **2008**, *130*, 5620. (b) Norako, M. E.; Franzman, M. A.; Brutchey, R. L. *Chem. Mater.* **2009**, *21*, 4299. (c) Norako, M. E.; Brutchey, R. L. *Chem. Mater.* **2010**, *22*, 1613. (d) Guo, Q.; Kim, S. J.; Kar, M.; Shafarman, W. N.; Birkmire, R. W.; Stach, E. A.; Agrawal, R.; Hillhouse, H. W. *Nano Lett.* **2008**, *8*, 2982. (e) Wang, Y.-H. A.; Zhang, X.; Bao, N.; Lin, B.; Gupta, A. *J. Am. Chem. Soc.* **2011**, *133*, 11072.
- (10) Lu, X.; Zhuang, Z.; Peng, Q.; Li, Y. *Chem. Commun.* **2011**, 3141.
- (11) (a) Franzman, M. A.; Perez, V.; Brutchey, R. L. *J. Phys. Chem. C* **2009**, *113*, 630. (b) Franzman, M. A.; Brutchey, R. L. *Chem. Mater.* **2009**, *21*, 1790. (c) Webber, D. H.; Brutchey, R. L. *Chem. Commun.*

2009, 5701. (d) Webber, D. H.; Brutchey, R. L. *Inorg. Chem.* **2011**, *50*, 723.

(12) (a) Li, Y.; Li, X.; Yang, C.; Li, Y. *J. Phys. Chem. B* **2004**, *108*, 16002. (b) Nose, K.; Soma, Y.; Omata, T.; Otsuka-Yao-Matsuo, S. *Chem. Mater.* **2009**, *21*, 2607. (c) Mahler, B.; Lequeux, N.; Dubertret, B. *J. Am. Chem. Soc.* **2010**, *132*, 953.

(13) (a) Pokrop, R.; Pamula, K.; Deja-Drogomirecka, S.; Zagorska, M.; Borysiuk, J.; Reiss, P.; Pron, A. *J. Phys. Chem. C* **2009**, *113*, 3487.

(b) Haram, S. K.; Quinn, B. M.; Bard, A. J. *J. Am. Chem. Soc.* **2001**, *123*, 8860.

(14) (a) Scragg, J. J.; Dale, P. J.; Peter, L. M.; Zoppi, G.; Forbes, I. *Phys. Status Solidi B* **2008**, *245*, 1772. (b) Ye, H.; Park, H. S.; Akhavan, V. A.; Goodfellow, B. W.; Panthani, M. G.; Korgel, B. A.; Bard, A. J. *J. Phys. Chem. C* **2011**, *115*, 234. (c) Riha, S. C.; Fredrick, S. J.; Sambur, J. B.; Liu, Y.; Prieto, A. L.; Parkinson, B. A. *ACS Appl. Mater. Interfaces* **2011**, *3*, 58.